Supporting information

p-Type Conductivity of Hydrated Amorphous V_2O_5 and its Enhanced Photocatalytic Performance in ZnO/V_2O_5/rGO

Heechae Choi,[1,‡] Yong Jung Kwon,[2,‡] Juwon Paik,[2] Jae-Bok Seol[3] and Young Kyu Jeong[2,*]

[1]Theoretical Materials & Chemistry Group, Institute of Inorganic Chemistry, University of Cologne, Greinstr. 6, 50939, Cologne, Germany

[2]Non-Ferrous Materials Group, KITECH, Gangneung 25440, South Korea

[3]National Institute for Nanomaterials Technology, POSTECH, Pohang 37673, South Korea

*Corresponding author. E-mail address: immrc80@gmail.com (Y. K. Jeong)

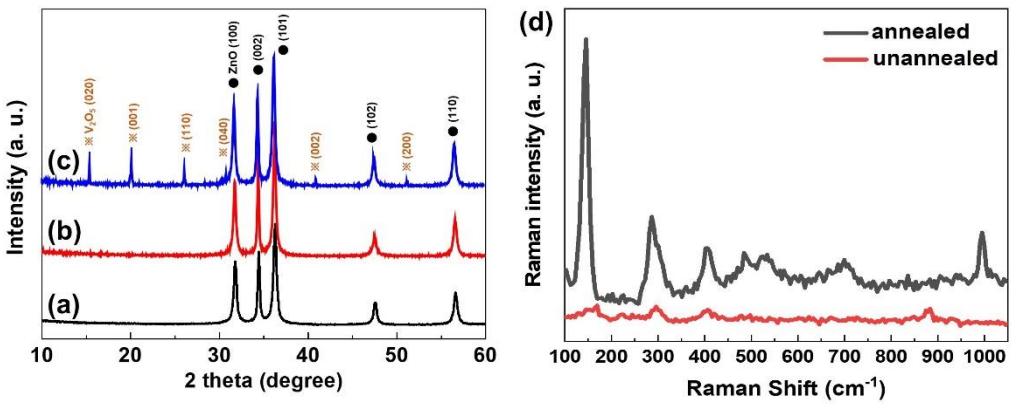

Figure S1. XRD patterns of (a) FLZ, (b) FLZ/*ha*-V_2O_5 and (c) FLZ/*c*-V_2O_5. (d) Raman spectra of annea led FLZ/*c*-V_2O_5 and unannealed FLZ/*ha*-V_2O_5 structures, respectively.

Figure S1(a) shows an XRD pattern of FLZ, exhibiting reflection peaks that can be indexed to the ZnO phase (JCPDS card: No. 36-1451). Also, the XRD spectra of FLZ/*ha*-V_2O_5 in Figure S2(b) show only the peaks of the ZnO phase without the peak associated with V_2O_5 phase. This result demonstrates that the unannealed *ha*-V_2O_5 shell layer is apparently amorphous. On the other hand, in figure S1(c), the XRD spectra of the FLZ/*c*-V_2O_5 exhibits ZnO-related peaks and also shows the reflections of V_2O_5 phase with a lattice parameter of a =1.1516 nm, b = 0.35656nm, and c = 0.4372 nm (JCPDS: 41-1426), indicating that the *ha*-V_2O_5 shell layers was crystallized by thermal annealing process.

Figure S1(d) shows a Raman spectra of annealed FLZ/*c*-V_2O_5 and unannealed FLZ/*ha*-V_2O_5 structures, respectively. Annealed V_2O_5 exhibits sharp bands reflecting its ordered crystal structure. The sharp Raman band at 995 cm^{-1} stems from vibration of the V=O double bond and the remaining bands from 200–800 cm^{-1} correspond to various vibrations of bridging V–O–V bonds of crystalline V_2O_5. In contrast to the sharp characteristics of Raman bands in the annealed V_2O_5, the unannealed one doesn't show the bands of crystalline V_2O_5 and possess broad bands implying the absence of long-range order.

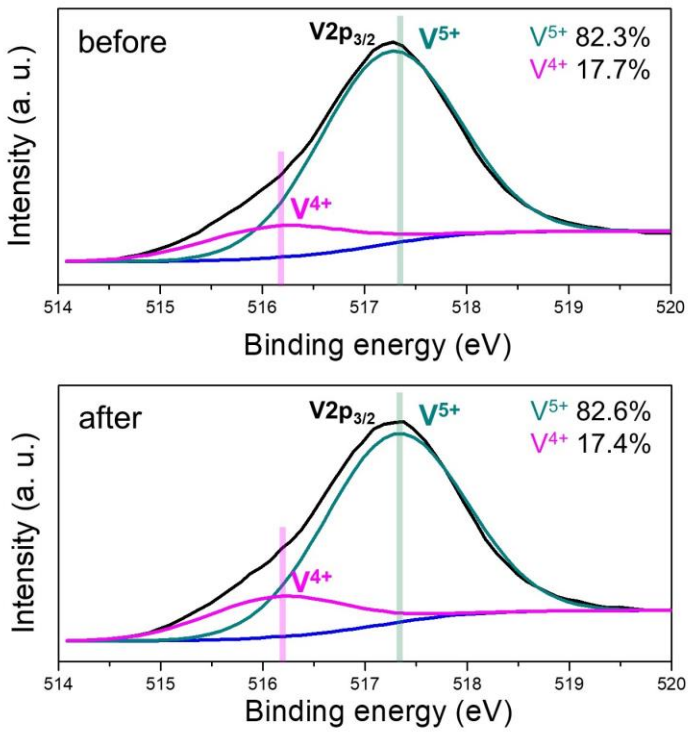

Figure S2. XPS V2p spectra of V_2O_5 before (top) and after (bottom) the RhB degradation test.

In order to confirm any compositional changes or contaminations of *ha*-V_2O_5 in the FLZ/*ha*-V_2O_5/rGO system during the photocatalytic experiments, we have performed XPS analysis. Figure S2 shows the V 2p spectra of V_2O_5 before and after the RhB degradation test. The XPS spectra show two peaks that correspond to V^{4+} and V^{5+}, respectively, indicating V_2O_5 dominantly consist of V_2O_5 compound with a small portion of VO_2. In addition, the two peaks were found to be almost identical suggesting that there are no significant changes in the chemical state and composition of V_2O_5. These XPS results additionally support the enhanced chemical stability of V_2O_5 by applying the rGO matrix in the FLZ/*ha*-V_2O_5/rGO system.

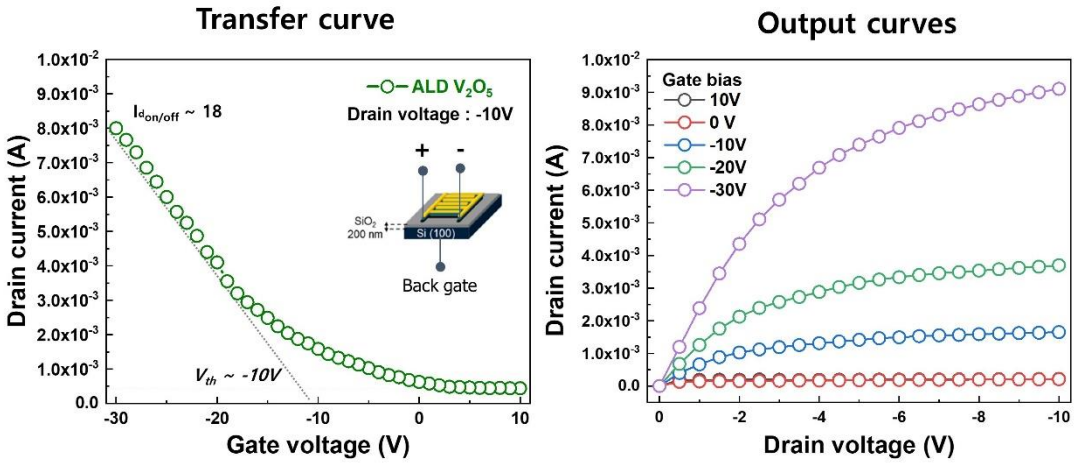

Figure S3. Electric characterizations of p-type ALD V_2O_5 layer which shows p-type behaviors in transfe r & output curves at room temperature.

We investigated its electric transport properties by fabricating a field-effect transistor (FET) which uses *ha*-V_2O_5 as a channel layer with back gate structures in order to study the conducting behavior of *ha*-V_2O_5 at room temperature. This device has a channel length of 10 μm and a dielectric (SiO_2) thick-ness of 200 nm. As shown in the transfer and output curves, the transfer and output curves of the *ha*-V_2O_5 FET clearly show typical p-type characteristics at room temperature.